

## Generalized Route to Metal Nanoparticles with Liquid Behavior

Scott C. Warren,<sup>†,‡</sup> Matthew J. Banholzer,<sup>†</sup> Liane S. Slaughter,<sup>†</sup> Emmanuel P. Giannelis,<sup>‡</sup>  
Francis J. DiSalvo,<sup>†</sup> and Ulrich B. Wiesner<sup>\*,‡</sup>

Department of Chemistry & Chemical Biology and Department of Materials Science & Engineering,  
Cornell University, Ithaca, New York 14853

Received June 23, 2006; E-mail: ubw1@cornell.edu

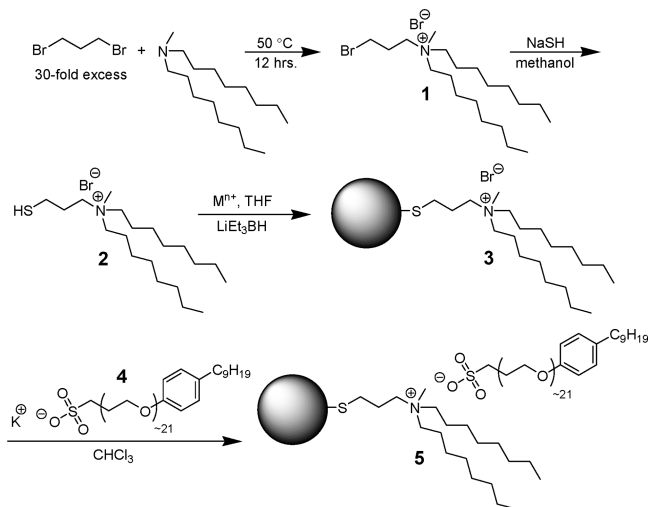
Most metals, especially transition metals, must be heated above 1000 °C to flow as a liquid.<sup>1</sup> This basic physical property of metals has strongly influenced the range of applications for this broad class of materials. At the same time, the high melting point has severely limited the ways that many metals can be handled and used. For example, it is unlikely that molten platinum will be cast in a rubber mold or used as a solvent for organic reactions. Here, we demonstrate that metals can be made to flow like liquids at room temperature by attaching an appropriate ligand to a metal nanoparticle. This new class of materials allows metals to be handled, assembled, and used in ways not previously possible. Furthermore, since the dynamics of nanoparticle flow contribute favorably to the thermal conductivity<sup>2</sup> and the fully accessible phonon modes of the metal increase the heat capacity of the liquid,<sup>3</sup> such materials may be of interest in heat-transfer fluids.

Numerous strategies for metal and ceramic nanoparticle functionalization have been explored. Although thiol-containing polymers,<sup>4,5</sup> ionic liquids,<sup>6</sup> and amphiphilic molecules<sup>7</sup> have been attached to metal nanoparticles previously, liquid-like properties have not been reported. In the case of ceramic nanoparticles, Giannelis et al. have demonstrated liquid-like properties when a silicon alkoxide with a quaternized ammonium was covalently attached to the nanoparticle surface.<sup>8–10</sup>

We synthesized the thiol *N,N*-dioctyl-*N*-(3-mercaptopropyl)-*N*-methylammonium bromide (**2**) in a simple, two-step process (Scheme 1). Reaction of excess 1,3-dibromopropane with *N,N*-dioctyl-*N*-methylamine, followed by vacuum distillation of the excess 1,3-dibromopropane, afforded **1** in 92% yield. The remaining 8% comprised the  $\beta$ -hydrogen rearrangement products *N,N*-dioctyl-*N*-methylammonium bromide and allyl bromide; the allyl bromide was removed during vacuum distillation. Upon dissolving the product in methanol, we added sodium hydrosulfide incrementally and stirred the solution at room temperature. Removal of methanol and dissolution in chloroform precipitated the sodium bromide and excess sodium hydrosulfide, which were removed by filtration. Evaporation of the chloroform in vacuo afforded a product mixture that included the thiol **2** (43%), the disulfide of **2** (35%), the sulfide of **2** (14%), and the side product from the previous reaction, *N,N*-dioctyl-*N*-methylammonium bromide (8%). This mixture required no further purification, as the thiol (and possibly the disulfide)<sup>11</sup> preferentially ligated to the nanoparticle surface and the side products were removed during nanoparticle purification.

To synthesize 2.0 nm platinum nanocrystals,<sup>12</sup> 0.300 g of H<sub>2</sub>-PtCl<sub>6</sub>·6H<sub>2</sub>O, 0.227 g of **2**, and 18 g of anhydrous THF were stirred for 30 min at 20 °C. We injected 10 mL of 1.0 M superhydride in THF at a constant rate over 10 s. After the solution was stirred for 30 min, a small amount of 2-propanol was added to quench any excess superhydride. Rotary evaporation to remove THF, followed

**Scheme 1.** Synthesis of Liquid Metal Nanoparticles



by centrifugation in methanol and then 90:10 water/methanol, afforded the pure product **3**, a powdery solid. This synthetic approach was generalized to gold, palladium, and rhodium nanoparticles (Supporting Information).

We examined **3** and **5** by TEM (Figure 1), PXRD (Figure 2), DSC, NMR, and TGA (Supporting Information). TEM and PXRD revealed that the gold and platinum particles had a high degree of crystallinity, while the palladium and rhodium nanoparticles were predominantly amorphous. Figure 1C,D demonstrates the ability to tune nanoparticle size by varying synthesis conditions, e.g., the reaction temperature or the injection rate of superhydride (Supporting Information). NMR revealed successful removal of all unwanted organic compounds, as the only organic material present is **2** bound to the nanoparticle surface. In both <sup>1</sup>H and <sup>13</sup>C NMR, the peak width increased upon nanoparticle ligation, and the methylene resonances closest to the thiol disappeared completely, as expected.<sup>13</sup>

To generate nanoparticles with liquid-like properties, sulfonate **4** was added to **3** to achieve a 1:1 bromide:sulfonate molar ratio (Supporting Information). After the solution was stirred in chloroform for several hours, water was added and stirring was continued for several more hours. Upon removal of the water by pipet, the chloroform was distilled off under vacuum to afford **5**. Vacuum reached <0.05 mbar, and analysis of **5** by NMR and TGA showed no residual solvent. These nanoparticles exhibited liquid-like flow at room temperature, as shown in Figures 3 and 4. The nanoparticle liquid was viscous, and the 50 mg drop moved 1.3 cm along an inclined glass plane over 30 min. DSC of the 2.0 nm platinum nanoparticles **5** (Figure 3) revealed that the ligands crystallize at -11 °C and melt at 16 °C (using a scan rate of 10 °C/min). A comparison between **4** and **5** revealed that the enthalpy

<sup>†</sup> Department of Chemistry & Chemical Biology.

<sup>‡</sup> Department of Materials Science & Engineering.

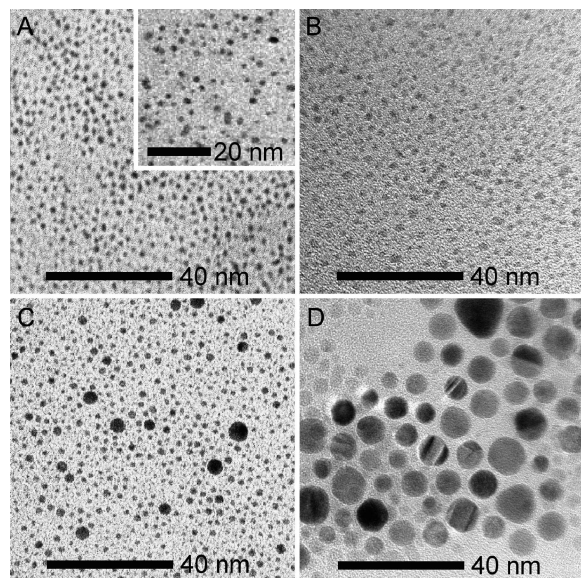


**Figure 1.** TEM micrographs of (A)  $2.0 \pm 0.3$  nm Pt, (B)  $1.7 \pm 0.4$  nm Pd, (C)  $2.5 \pm 0.8$  nm Au, and (D)  $7.9 \pm 3.0$  nm Au. All micrographs are of **3** except for the inset of (A), which shows  $2.0 \pm 0.4$  nm Pt nanoparticles **5**.

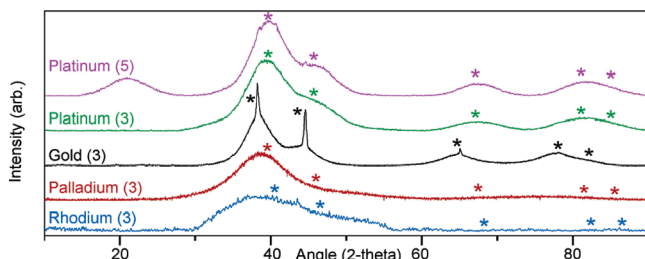


**Figure 2.** PXRD traces of 2.0 nm platinum nanoparticles (1.2 nm domain size), 2.5 nm gold nanoparticles (2.4 nm domain size), 1.7 nm palladium particles (slightly crystalline), and 2.0 nm rhodium nanoparticles (mostly amorphous). Expected peaks are labeled with asterisks. Nanoparticles with bromide anions (**3**) show scattering only from the metal, but conversion to **5** reveals scattering from the sulfonate anion at  $20^\circ$ . The sharp peaks of gold arise from the small number of larger nanoparticles.

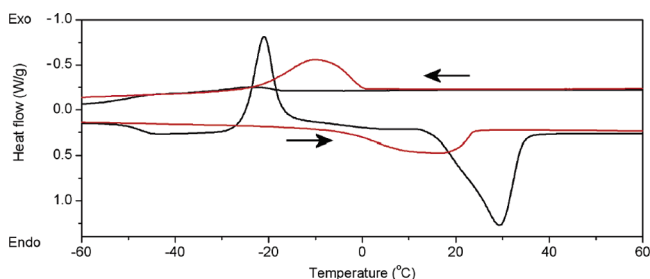


**Figure 3.** DSC trace of sulfonate **4** (black trace) and 2.0 nm liquid platinum nanoparticles **5** (red trace).

of melting for **5** was half that of **4**, which is consistent with the fact that **5** was synthesized by combining equal masses of **3** and **4**.

Several trends were apparent from TGA measurements of **3** and **5**. In general, the mass loss observed in TGA measurements depended on metal density (mass loss of Pd > Pt), nanoparticle size (mass loss of 2.0 nm Pt > 2.7 nm Pt), counterion (mass loss of sulfonate > bromide), and sample purity. Additionally, the nanoparticles achieved greater thermal stability upon conversion

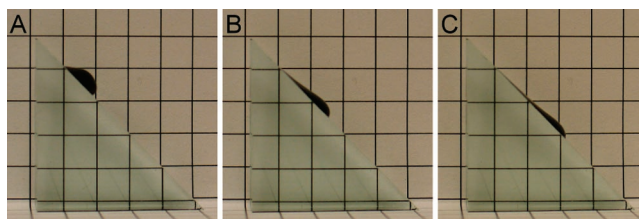


**Figure 4.** Time series of a 50 mg drop of  $2.0 \pm 0.3$  nm platinum nanoparticles **5** flowing down a  $45^\circ$  glass slope. With respect to the photograph in (A), images were taken after (B) 2 min and (C) 8 min. Each grid is 5 mm on a side.

from **3** to **5**, with the onset of decomposition rising by  $26^\circ\text{C}$ , on average. However, the onset of decomposition still occurred at relatively low temperatures for **5**, ranging from  $151^\circ\text{C}$  for rhodium to  $220^\circ\text{C}$  for 2.5 nm gold. This is likely due to the catalytic role of late transition metals in hydrocarbon combustion. TGA also revealed the area density of ligands on the nanoparticle surfaces. The ligand density of **3** typically ranged from 0.22 to  $0.26\text{ nm}^2/\text{ligand}$ , which was slightly higher than the  $0.21\text{ nm}^2/\text{ligand}$  of linear alkanethiols on 2.8 nm gold nanoparticles.<sup>4</sup> This difference is likely related to steric repulsion between neighboring thiols on the nanoparticle surface.

In summary, we have developed a generalized route to metal nanoparticles in which a thiol-containing ionic liquid serves as a ligand for platinum, gold, palladium, and rhodium nanoparticles. Upon anion exchange of bromide for sulfonate, the nanoparticles flow as a liquid at room temperature. We expect this development will open new routes to self-assembled hybrids and may have application, e.g., in the area of heat-transfer fluids.

**Acknowledgment.** This work was supported by grants from the DOE and the NSF, through the Cornell Center for Materials Research. S.C.W. acknowledges support from the Environmental Protection Agency STAR fellowship program. The authors thank Peter Ercius and John Grazul for assistance with HRTEM.

**Supporting Information Available:** Experimental procedures and characterization of new compounds and materials. This material is available free of charge via the Internet at <http://pubs.acs.org>.

## References

- (1) *CRC Handbook of Chemistry and Physics*, 86th ed.; Lide, D. R., Ed.; CRC Press: Cleveland, OH, 2005.
- (2) Koblinski, P.; Eastman, J.; Cahill, D. *Mater. Today* **2005**, *8* (6), 36–44.
- (3) Ashcroft, N. W.; Mermin, N. D. *Solid State Physics*; Holt, Rinehart, and Winston: New York, 1976.
- (4) Wuelfing, W. P.; Gross, S. M.; Miles, D. T.; Murray, R. W. *J. Am. Chem. Soc.* **1998**, *120*, 12696–12697.
- (5) Teranishi, T.; Kiyokawa, I.; Miyake, M. *Adv. Mater.* **1998**, *10*, 596–599.
- (6) Kim, K.; Demberelnyamba, D.; Lee, H. *Langmuir* **2004**, *20*, 556–560.
- (7) Zubarev, E. R.; Xu, J.; Sayyad, A.; Gibson, J. D. *J. Am. Chem. Soc.* **2006**, *128*, 4958–4959.
- (8) Bourlinos, A. B.; Herrera, R.; Chalkias, N.; Jiang, D. D.; Zhang, Q.; Archer, L. A.; Giannelis, E. P. *Adv. Mater.* **2005**, *17*, 234–237.
- (9) Bourlinos, A. B.; Chowdhury, S. R.; Herrera, R.; Jiang, D. D.; Zhang, Q.; Archer, L. A.; Giannelis, E. P. *Adv. Funct. Mater.* **2005**, *15*, 1283–1290.
- (10) Bourlinos, A. B.; Chowdhury, S. R.; Stassinopulos, A.; Anglos, D.; Herrera, R.; Anastasiadis, S. H.; Petridis, D.; Giannelis, E. P. *Small* **2006**, *4*, 513–516.
- (11) Porter, L. A.; Ji, D.; Westcott, S. L.; Graupe, M.; Czernuszewicz, R. S.; Halas, N. J.; Lee, T. R. *Langmuir* **1998**, *14*, 7378–7386.
- (12) Eklund, S. E.; Cliffel, D. E. *Langmuir* **2004**, *20*, 6012–6018.
- (13) Song, Y.; Harper, A. S.; Murray, R. W. *Langmuir* **2005**, *21*, 5492–5500.

JA064469R